UNEXPECTED OBSERVATIONS ON THE ACCURACY OF LINEAR COVARIANCE ANALYSIS AND TRACK ASSOCIATION

Alexandra H. Nelson[*], Jackson Kulik [†]

This paper presents two unexpected findings related to the accuracy of linear covariance propagation in astrodynamics. First, higher-dimensional state distributions experience a more rapid deviation from Gaussianity than lower dimensional marginal distributions; in particular, 6-dimensional states diverge from Gaussian behavior significantly faster than 2- or 3-dimensional states. This effect is quantified, and the paper provides information on its underlying causes. Second, it was found that increasing the initial covariance can, in some cases, reduce the non-Gaussianity of the propagated distribution. This counterintuitive behavior is examined in detail, and possible explanations are discussed.

INTRODUCTION

Accurately quantifying and modeling the covariance associated with a spacecraft state is crucial in applications where a spacecraft state needs to be known precisely. This includes space domain awareness (SDA), rendezvous proximity operations (RPO), track association, navigation filters, and many other related applications. In these applications non-precise covariance models can lead to overconfidence in the spacecrafts predicted state and ultimately mission failure.

This paper discusses two anomalies related to linear covariance propagation techniques. These anomalies were studied in the context of track association, but the findings are applicable to various other scenarios.

Linear covariance propagation is a technique commonly used in spacecraft applications to propagate the covariance associated with a state forward in time.[1] Given a mean initial state $\boldsymbol{\mu}_x$ and a previously known covariance $\mathbf{P}(0)$ the solution to the dynamical system φ_t can be computed for a given state $\mathbf{x}(t)$ as shown in Eq. 1.

$$\varphi_t(\mathbf{x}(0)) = \mathbf{x}(t) \tag{1}$$

The Jacobian of the solution φ_t evaluated at the mean initial state is the state transition matrix $\mathbf{\Phi}$ and can be calculated as shown in Eq. 2.

$$\mathbf{\Phi}(t, t_0) = \left.\frac{\partial \varphi_t}{\partial \mathbf{x}(t)}\right|_{\boldsymbol{\mu_x}(t_0)} \tag{2}$$

[*]PhD Student, Mechanical and Aerospace Engineering, Utah State University, Logan UT
[†]Assistant Professor, Mechanical and Aerospace Engineering, Utah State University, Logan UT

The state transition matrix and the initial covariance can then be used to propagate the covariance as shown in Eq. 3.

$$\mathbf{P}(t) = \mathbf{\Phi}(t, t_0)\mathbf{P}(0)\mathbf{\Phi}(t, t_0)^{\mathbf{T}} \tag{3}$$

Since only linear terms are included in the state transition matrix, the covariance is a linear approximation of the actual covariance. This approximation is appropriate for some space applications, but it introduce error. The Gaussian distribution obtained from the linear covariance approximation becomes a less accurate approximation of the true distribution.

Several previous studies quantitatively discuss how non-Gaussian the distribution becomes using both Monte Carlo methods and analytical approaches.[2–4] In addition, nonlinear uncertainty propagation methods have been developed, such as the gaussian mixture method for uncertainty propagation,[5] polynomial chaos expansion,[6] state transition tensors,[7] unscented transforms,[8] conjugate unscented transformation,[9] and differential algebra.[10]

This paper discusses two unexpected findings that were observed while exploring methods to better perform track association. The first observation was that the non-Gaussianity of the distribution changed with the dimension of the distribution. When the full 6-dimensional state was considered, the non-Gaussianity increased much faster than when a subset of the state variables were considered. As a result, the non-Gaussianity manifests to different degrees in the full distribution as opposed to lower dimensional marginal distributions.

The second unexpected finding is that the non-Gaussianity did not always increase as the initial covariance increased. If the initial uncertainty was higher, one would expect that the non-Gaussianity of the distribution at a later time would also be higher. However, it was observed that inflating the initial covariance in certain ways resulted in a more Gaussian distribution, and linear covariance propagation gave better results under a number of different metrics for identifying non-Gaussianity.

BACKGROUND

Covariance based track association with a Chi-squared test

To determine if a d-dimensional measurement is statistically consistent with a distribution for the spacecraft's state, a chi-squared test can be performed. A chi-squared test examines the squared Mahalanobis distance D^2 between the measurement and the measurement function applied to the mean of the state distribution. This squared Mahalanobis distance is compared with the chi-squared value $\chi^2_{\alpha,d}$ of the estimated state of the spacecraft, given a significance value α and degrees of freedom d. When calculating the Mahalanobis distance, $\mathbf{x}$ or some subset of $\mathbf{x}$ is the measurement, $\boldsymbol{\mu}$ is the estimated state of the spacecraft at the time of the measurement, and $\mathbf{P}$ is the estimated covariance of the spacecraft at the time of the measurement. In the context of this work, the measurement gives the full spacecraft state. When marginal distributions are considered the measurement gives the appropriate marginal spacecraft state.

$$D^2 = (\mathbf{x} - \boldsymbol{\mu_x})^{\mathbf{T}}\mathbf{P_t}^{-\mathbf{1}}(\mathbf{x} - \boldsymbol{\mu_x}) \tag{4}$$

Comparison of Mahalanobis distance and chi-squared value determines if the measurement is consistent with a distribution.

Hypothesis Test

- If $D^2 > \chi^2_{\alpha,p}$, the observation is inconsistent with the expected distribution.
- If $D^2 \leq \chi^2_{\alpha,p}$, the observation is not inconsistent with the expected distribution.

If the measurement is consistent with the distribution, we do not reject the null hypothesis that the measurement is associated with the given distribution. If the measurement is not consistent with the distribution, we reject the null-hypothesis that this measurement is associated with the given distribution.

Chi-squared tests work if the state has a multivariate normal distribution. This results in the squared Mahalanobis distance having a chi-squared distribution. However, as the distribution becomes less gaussian the accuracy of the chi-squared test also decreases.

TODO:: This paper will discuss the use of the chi-squared test in the Jenson and Scheeres paper as a measure of non-Gaussianity rather than explicitly for track association.[4]

A Measure of Non-Gaussianity: WUSSOS

The whitened uncertainty-scaled second-order stretching (WUSSOS) metric is an empirical method used to quantify error that results from linear covariance propagation.[2] WUSSOS uses a whitening transformation on the higher-order terms of the flow map. The Taylor series expansion for the flow map can be seen in Eq. 5.

$$\mathbf{g}(\boldsymbol{\mu_x} + \delta\mathbf{x}) = \mathbf{g}(\boldsymbol{\mu_x}) + \mathbf{G}\,\delta\mathbf{x} + \frac{1}{2}\left.\frac{\partial^2 \mathbf{g}}{\partial \mathbf{x}^2}\right|_{\boldsymbol{\mu_x}} \delta\mathbf{x}^2 + \mathcal{O}(\delta\mathbf{x}^3) \tag{5}$$

The second order terms of this expansion are denoted as $\boldsymbol{\Psi}$ as shown in Eq. 6.

$$\boldsymbol{\Psi} = \left.\frac{\partial^2 \mathbf{g}}{\partial \mathbf{x}^2}\right|_{\boldsymbol{\mu_x}} \tag{6}$$

Then WUSSOS requires an optimization to determine the maximal error in propagating the vectors on the 1-sigma initial covariance ellipsoid relative to the covariance as propagated by linear covariance analysis. The equation for WUSSOS is shown in Eq (7)

$$\max_{\mathbf{x}^T \mathbf{P}(0)^{-1} \mathbf{x} = 1} \left\| \boldsymbol{\Psi}\mathbf{x}^2 \right\|_{\mathbf{P}(t)^{-1}} \tag{7}$$

where $\boldsymbol{\Psi}\mathbf{x}^2$ is shorthand notation for the double contraction of the tensor using Einstien notation. This can be seen in Eq. 8

$$\left(\boldsymbol{\Psi}\mathbf{x}^2\right)^i = (\boldsymbol{\Psi})^i_{j,k}\ \mathbf{x}^j \mathbf{x}^k \tag{8}$$

The WUSSOS value can be used to determine the relative non-Gaussianity of the distribution over time because it is an uncertainty scaled measure of the difference between the first and second order approximations.

TODO:: This paper will include a discussion on Position WUSSOS

CASE STUDIES

Dimensionality

To explore the non-gaussianity of a full state distribution with a lower-dimensional marginal distribution, we followed the procedure used by Gutierrez et. al.[4] to quantify non-gaussianity of a propagated distribution. Ten-thousand random samples were generated for the initial state and covariance shown in Eq. (9). These initial conditions for the mean represent a spacecraft in an equatorial circular orbit with a radius of 6678.0 km.

$$\begin{aligned} \mathbf{x}(0) &= [6678.0\text{km},\ 0\text{km},\ 0\text{km},\ 0\text{km/s},\ \sqrt{\frac{\mu}{6678.0}}\text{km/s},\ 0\text{km/s}] \\ \mathbf{P}(0) &= \text{diag}([0.01\text{km},\ 0.01\text{km},\ 0.01\text{km},\ 10^{-6}\text{km/s},\ 10^{-6}\text{km/s},\ 10^{-6}\text{km/s}]) \end{aligned} \tag{9}$$

where μ is the gravitational parameter $398600.0\text{km}^2/\text{s}^2$.

The mean state and the samples were propagated forward in time using two-body dynamics with no perturbations. The covariance was propagated using linear covariance propagation as shown in Eq. 3 . Then, a chi-squared test associated with the distribution propagated with linear covariance analysis was performed at each time for each propagated sample.

The chi-squared test was performed with the full state vectors as well as with projections of the state into lower dimensions. A threshold of 98.8%, the 3-sigma bound associated with 2-dimensional gaussian random variable, was applied to each chi-squared test. Since the samples came from the initial state distribution, if the linear covariance propagation is entirely accurate in describing the distribution at later time steps and a threshold of 98.8% is used, it is expected that approximately 98.8% of the samples will pass the chi-squared test. The deviation in the number of propagated samples passing the chi-squared test from this anticipated value gives a measure of the effectiveness of the linear covariance propagation and the resulting non-gaussianity of the true nonlinearly propagated distribution.

The results of these chi-squared tests over time are shown in Fig. 1. All dimensions begin with 98.8% of the samples passing the chi-squared test and being associated with the linear covariance distribution. As the orbit progresses, the percentage of samples associated with the linear covariance distribution decreases. This is expected, as linear covariance propagation becomes a poor approximation for nonlinear systems over time.

An interesting aspect of Fig. 1 is the varying rate at which the percentage of samples associated with the mean decreases. Fig. 1 shows that linear covariance propagation provides a better approximation for lower-dimensional states (2 or 3 dimensions), but the accuracy decreases as the state dimensionality increases.

Next, various permutations of 2D states were studied (e.g., x and y, x and z, x and $\dot{x}$ ...). The 2-dimensional case was chosen due to the in-plane motion of the orbit; if out-of-plane motion is present, a 3-dimensional state representation might be more appropriate. The results of this study are shown in Fig. 2. Note that only the permutations including x are shown in the graph. Other permutations were examined, but the results were very similar, so only the x-based permutations are shown for clarity.

This study confirmed that the results in Fig. 1 were not due to a random permutation of states. All 2-dimensional permutations exhibit a slower decrease in accuracy compared to the 6-dimensional

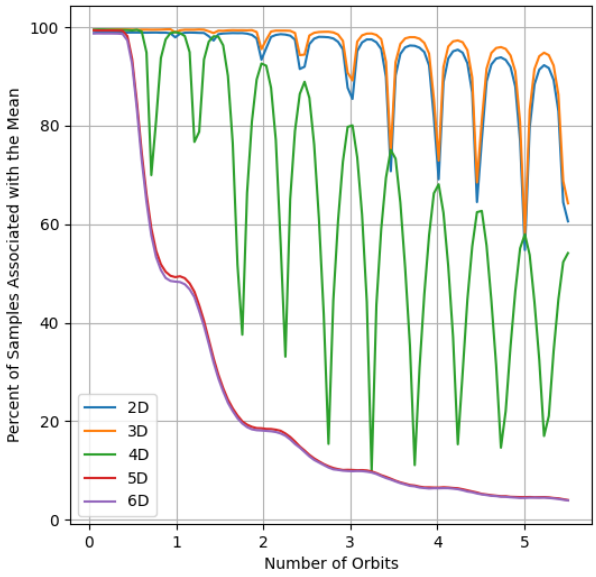

Figure 1. Chi-Squared results for different state dimensions.

state.

TODO:: WUSSOS metric will be used to analyze the dimensionality results.

TODO:: An explanation of why this occurs will be included

- delta spherical shell includes more area in higher dimensions
- Expected Squared Mahalanobis Distance of Linearization Error and graphs[2]

This result suggests that care must be taken when applying linear covariance propagation to high-dimensional systems. If computational constraints allow, lower-dimensional projections or nonlinear methods may yield more reliable statistical consistency.

Initial Covariance Affect on Non-Gaussianity

Surprisingly, increasing the initial covariance sometimes results in a higher percentage of samples passing the chi-squared test, indicating that linear covariance propagation is more accurate with higher initial uncertainties. The same methodology used in the dimensionality study was applied to a fixed 6-dimensional mean state. This time, the marginal standard deviation for all position components was varied from 0.01 km to 100.0 km as a part of a diagonal covariance matrix. This same graph was then produced using 2-dimensional marginal positions in the x-y plane. Both graphs can be seen in Fig. 3

In the 6-dimensional plot, a smaller initial position uncertainty of 0.01 km led to inferior chi-squared test performance compared to a 1.0 km uncertainty. This was an unexpected result given the conventional assumption that smaller uncertainties produce more reliable results under linear

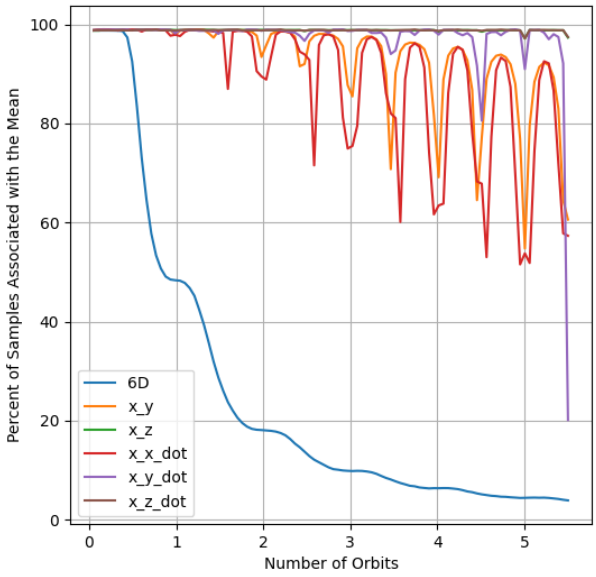

Figure 2. Chi-Squared results for different 2-dimensional states.Illustration Caption Goes Here

approximation. To further investigate, a similar analysis was performed using 2-dimensional state projections. This helped isolate whether the effect was related to state dimensionality or a more general property of the dynamics. The 2-dimensional plot showed that overall linear covariance results performed as expected but at half and full orbits the higher initial position covariance of 1.0 km and 0.1 km performed better than the 0.01 km initial position covariance.

To further explore this effect, WUSSOS values — an uncertainty scaled measure of second-order nonlinearity — were computed for each case. The results of this study are shown in Fig. 4. The WUSSOS plots revealed anomalous behavior at approximately half and full orbital periods, where increased initial covariance did not correspond to higher maximum nonlinearity, contrary to expectations.

TODO:: Create Position WUSSOS plot

This unexpected observation is the result of singularities associated with these times of flight. Previous work discusses these singularities in a variety of different contexts.[11–13] In this paper, the singularity is the result of the covariance, associated with the velocity, dominating and causing the covariance matrix to be singular as shown in Eq. 10.

$$\mathbf{P}(0) = \begin{bmatrix} \mathbf{P}_{rr} & \mathbf{0} \\ \mathbf{0} & \mathbf{P}_{vv} \end{bmatrix} \approx \begin{bmatrix} \mathbf{0} & \mathbf{0} \\ \mathbf{0} & \mathbf{P}_{vv} \end{bmatrix} \tag{10}$$

Using the covariance from Eq. 10 and the STM shown in Eq. 11 the covariance can be found using linear covariance propagation as shown in Eq. 12.

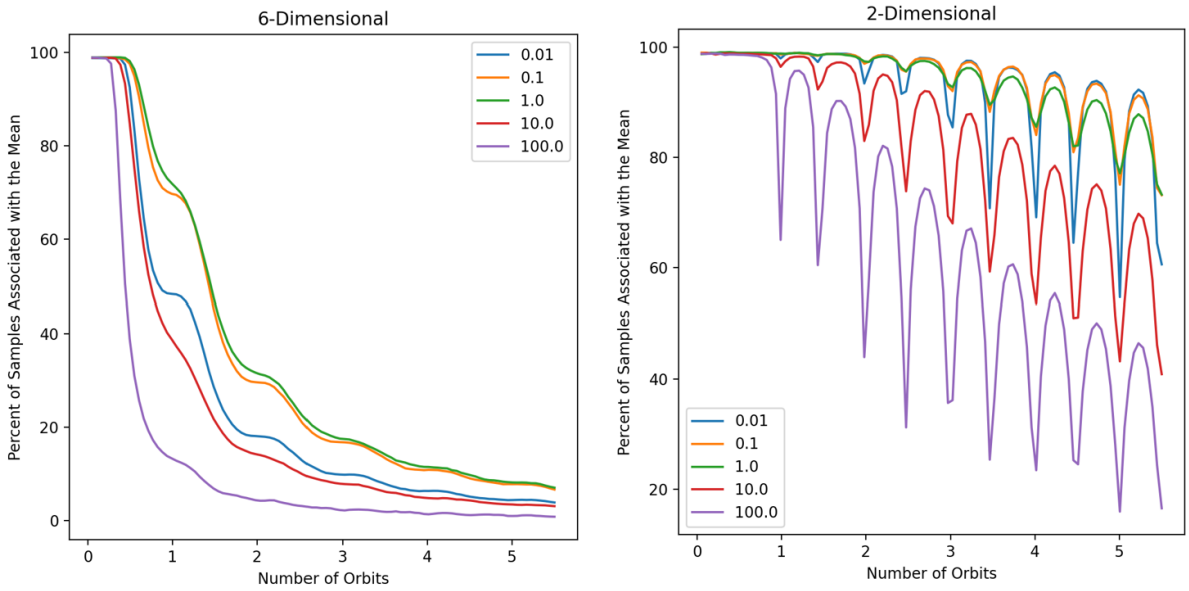

Figure 3. Chi-Squared results for different initial position covariances.

$$\mathbf{\Phi}(t, t_0) = \begin{bmatrix} \mathbf{\Phi}_{rr} & \mathbf{\Phi}_{rv} \\ \mathbf{\Phi}_{vr} & \mathbf{\Phi}_{vv} \end{bmatrix} \tag{11}$$

$$\mathbf{P_{rr}}(t) = \mathbf{\Phi_{rv}}(t, t_0)\mathbf{P_{vv}}(0)\mathbf{\Phi_{rv}}(t, t_0)^T \tag{12}$$

The singularities then occur when the determinate of the $\mathbf{\Phi_{rv}}$ is zero. These points are multiples of 2π and 1.4067, 2.4453, 3.4612, etc. These points are where we see higher initial uncertainties performing better than lower initial uncertainties.

This result suggests that in some orbital regimes, small initial uncertainties in marginal position may lead to deceptive confidence in the accuracy of linear propagation. The effect of singularities in blocks of the state transition matrix need to be considered when using linear covariance propagation with heteroscedastic initial uncertainty.

CONCLUSION

TODO:: A conclusion will be included after all results are finalized.

REFERENCES

[1] D. K. Geller, "Linear Covariance Techniques for Orbital Rendezvous Analysis and Autonomous Onboard Mission Planning," Vol. 29, No. 6, pp. 1404–1414, 10.2514/1.19447.

[2] J. Kulik, B. Hastings, and K. A. LeGrand, "LINEAR COVARIANCE FIDELITY CHECKS AND MEASURES OF NON-GAUSSIANITY,"

[3] P. Singla, M. Majji, and M. Mercurio, "How Non-Gaussian Is It?,"

[4] J. Gutierrez, K. Hill, E. L. Jenson, D. J. Scheeres, J. C. Bruer, and R. D. Coder, "Classifying State Uncertainty for Earth-Moon Trajectories," Vol. 71, No. 3, p. 29, 10.1007/s40295-024-00451-w.

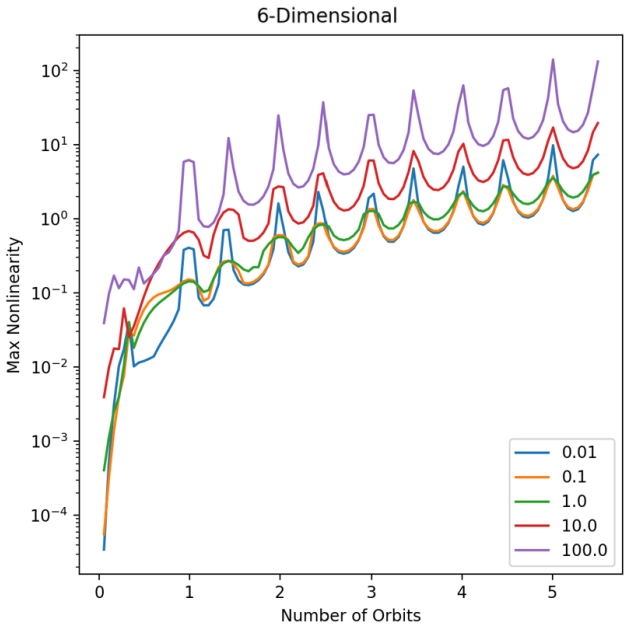

Figure 4. WUSSOS plots for varying initial position covariance.

[5] K. J. DeMars, R. H. Bishop, and M. K. Jah, "Entropy-Based Approach for Uncertainty Propagation of Nonlinear Dynamical Systems," Vol. 36, No. 4, pp. 1047–1057, 10.2514/1.58987.

[6] B. A. Jones, A. Doostan, and G. H. Born, "Nonlinear propagation of orbit uncertainty using non-intrusive polynomial chaos," *Journal of Guidance, Control, and Dynamics*, Vol. 36, No. 2, 2013, pp. 430–444.

[7] I. Park and D. J. Scheeres, "A HYBRID METHOD FOR UNCERTAINTY PROPAGATION OF ORBITAL MOTION AROUND THE EARTH,"

[8] S. J. Julier and J. K. Uhlmann, "Unscented filtering and nonlinear estimation," *Proceedings of the IEEE*, Vol. 92, No. 3, 2004, pp. 401–422.

[9] N. Adurthi, P. Singla, and T. Singh, "Conjugate Unscented Transformation: Applications to Estimation and Control," Vol. 140, No. 3, p. 030907, 10.1115/1.4037783.

[10] R. Armellin, P. Di Lizia, F. Bernelli-Zazzera, M. Berz, *et al.*, "Nonlinear mapping of uncertainties: a differential algebraic approach," *4th International Conference on Astrodynamics Tools and Techniques (ICATT)*, 2010, pp. 04–29.

[11] J. Kulik and D. Savransky, "Relative Transfer Singularities and Multi-Revolution Lambert Uniqueness," *AIAA SCITECH 2022 Forum*, American Institute of Aeronautics and Astronautics, 10.2514/6.2022-0958.

[12] F.-T. Sun, "On the Minimum Time Trajectory and Multiple Solutions of Lambert's Problem,"

[13] H. Chen, C. Han, Y. Rao, J. Yin, and X. Sun, "Algorithm of Relative Lambert Transfer Based on Relative Orbital Elements," Vol. 42, No. 6, pp. 1413–1422, 10.2514/1.G003348.